Atmospheric Environment 187 (2018) 50–61

Contents lists available at ScienceDirect

Atmospheric Environment

journal homepage: www.elsevier.com/locate/atmosenv

Ammonia emissions from biomass burning in the continental United States

Casey D. Bray[a,*], William Battye[a], Viney P. Aneja[a], Daniel Q. Tong[b,c,d], Pius Lee[b], Youhua Tang[b,c]

[a] North Carolina State University, Raleigh, NC 27695, United States
[b] NOAA Air Resources Laboratory, 5830 University Research Court, College Park, Maryland, MD 20740, United States
[c] Cooperative Institute for Climate and Satellites, University of Maryland, College Park, Maryland, MD 20740, United States
[d] Center for Spatial Information Science and Systems, George Mason University, Fairfax, Virginia, VA 22030, United States

ARTICLE INFO

Keywords:
Ammonia
Wildfires
Biomass burning
National emissions inventory
Fire emissions

ABSTRACT

This study quantifies ammonia (NH_3) emissions from biomass burning from 2005 to 2015 across the continental US (CONUS) and compares emissions from biomass burning with the US Environmental Protection Agency (EPA) National Emissions Inventory (NEI), the Fire Inventory from the National Center for Atmospheric Research (FINN) and the Global Fire Emissions Database (GFED). A statistical regression model was developed in order to predict NH_3 emissions from biomass burning using a combination of fire properties and meteorological data. Satellite data were used to evaluate the annual fire strength and frequency as well as to calculate the total NH_3 emissions across the CONUS. The results of this study showed the total fire number has decreased, while the total yearly burn area and the average fire radiative power has increased. The average annual NH_3 emissions from biomass burning from this study, on a national scale, were approximately 5.4e8 ± 3.3e8 kg $year^{-1}$. When comparing the results of this study with other emission inventories, it was found that ammonia emissions estimated by the NEI were approximately a factor of 1.3 lower than what was calculated in this study and a factor of 1.1 lower than what was modeled using the statistical regression model for 2010–2014. The calculated NH_3 emissions from biomass burning were a factor of 5.9 and a factor of 13.1 higher than the emissions from FINN and the GFED, respectively. The modeled NH_3 emissions from biomass burning were a factor of 5.0 and a factor of 11.1 higher than the emissions from FINN and the GFED, respectively. As the climate continues to change, the pattern (frequency, intensity and magnitude) of fires across the US will also change, leading to changes in NH_3 emissions. The statistical regression model developed in this study will allow prediction of NH_3 emissions associated with climate change.

1. Introduction

Ammonia (NH_3) is an important base gas in the atmosphere (Battye et al., 2017; Aneja et al., 1998, 2008). NH_3 reacts with sulfuric, nitric and hydrochloric acids to form ammonium sulfate, ammonium bisulfate, ammonium nitrate and ammonium chloride which contribute to the formation of $PM_{2.5}$ (particulate matter with diameter less than 2.5 micrometers) (Baek and Aneja, 2004; Baek et al., 2004; Davidson et al., 2011; Day et al., 2012; Chen et al., 2014). There are many adverse health effects associated with exposure to elevated concentrations of fine particulate matter, such as chronic bronchitis, aggravated asthma, irregular heartbeat, other cardiovascular and respiratory issues and even death (Pope et al., 2002, 2009; Schwartz et al., 2002; Kwok et al., 2013; Crouse et al., 2015; Lelieveld et al., 2015). Exposure to elevated $PM_{2.5}$ concentrations is a major concern for human health and welfare due to the particles' ability to penetrate deep into the respiratory tract. $PM_{2.5}$ is also associated with several environmental impacts, such as reducing visibility and changing the earth's radiational balance (Fan et al., 2005; Behera and Sharma, 2010a, 2010b; Heald et al., 2012; Wang et al., 2012). Furthermore, gaseous NH_3 may be deposited to the Earth's surface, which leads to ammonification, eutrophication and a loss of biodiversity (Langford et al., 1992; Robarge et al., 2002; Galloway et al., 2004; Clark and Tilman, 2008; Janssens et al., 2010; Day et al., 2012; Holtgrieve et al., 2011; Phoenix et al., 2012; Erisman et al., 2013; Chen et al., 2014). Increased concentrations of NH_3 can also lead to a decreased resistance to drought and frost damage (Robarge et al., 2002). In addition, NH_3 plays a role in the formation of nitrous oxide, which is a major greenhouse gas (Bouwman, 1996).

Major sources of atmospheric NH_3 include NH_3 based fertilizers, animal waste, and biomass burning, with intensely managed livestock and agricultural sources of NH_3 contributing most to NH_3 concentrations (Langford et al., 1992; Schlesinger and Hartley, 1992; Bouwman et al., 1997; Flechard and Fowler, 1998; Battye et al., 2003; Aneja et al.,

* Corresponding author.
E-mail address: cdbray@ncsu.edu (C.D. Bray).

https://doi.org/10.1016/j.atmosenv.2018.05.052
Received 24 December 2017; Received in revised form 16 May 2018; Accepted 26 May 2018
Available online 29 May 2018

2009; Zbieranowski and Aherne, 2012). While agriculture accounts for approximately 82% of all NH_3 emissions on a national level, fires account for a total of about 10% of all ammonia emissions nationwide (2014 NEI). NH_3 is mainly emitted into the atmosphere during smouldering combustion, which occurs in slow, low-temperature fires without a flame (Langford et al., 1992; Nance et al., 1993; Goode et al., 2000; McMeeking et al., 2009; Akagi et al., 2011; Alves et al., 2011; Chen et al., 2014).

Previous works have shown an overall increase in NH_3 sources (Erisman et al., 2008) and atmospheric NH_3 concentrations over the past several years (Saylor et al., 2015; Butler et al., 2016; Yao and Zhang, 2016). While the overall increase in NH_3 emissions cannot solely be attribute to fire activity, it is possible that biomass burning emissions of NH_3 are contributing to the observed increase in ambient emissions. For example, Saylor et al. (2015) also observed unusually high concentrations of NH_3 across the southeastern United States (US) during 2007, when fires were prevalent due to increased temperatures and widespread drought. Similarly, R'Honi et al. (2013) observed NH_3 concentrations were two orders of magnitude larger than background levels during the summer of 2010, which was the hottest and driest summer on record (until 2015), when wildfires ran rampant across Europe and Russia. Hot and dry conditions in the Mediterranean countries, Australia and the western United States have contributed to an increase in wildfire activity, thus increasing the emission of gaseous NH_3, among other pollutants, into the atmosphere (Alves et al., 2011). The strength and frequency of fires are not only controlled by the properties of the fuel and the geography, but they are also influenced by weather and climate (Pyne et al., 1996; Liu et al., 2010). Therefore, changes in the earth's climate will likely result in changes in fire activity. Higher temperatures and widespread drought are expected to cause an increase in the number of observed wildfires across many regions, such as the southeastern United States, the northern great plains, the Pacific coast, the southwestern US and the southern Rockies (Piñol et al., 1998; Gillett et al., 2004; Reinhard et al., 2005; Liu, 2006; Westerling et al., 2006; Alves et al., 2011; Litschert et al., 2012; Saylor et al., 2015; Skibba, 2015). However, due to changes in relative humidity and wind speeds, the future fire potential in the northern Rockies and the northwestern United States may likely be reduced (Liu et al., 2013). On a global scale, wildfire potential is projected to increase as the climate changes, specifically in locations that are already prone to the occurrence of wildfires (Liu et al., 2010). This increase in wildfire potential will then potentially lead to an increase in NH_3 emissions from biomass burning.

Biomass burning is an important source of NH_3 emissions, but the strength of the source remains poorly quantified (Alves et al., 2011; Chen et al., 2014). Therefore, the primary objective of this study is to quantify NH_3 emissions from biomass burning (wildfires, agricultural burns and prescribed burns) from 2005 to 2015 across the continental US and compare against major emission inventories used in atmospheric models. The inventories compared in this study include the Fire Inventory from the National Center for Atmospheric Research (FINN v1.5, Wiedinmyer et al., 2011), the Global Fire Emissions Databases (GFED v4.1, with small fires; Van Der Werf et al., 2017), and the US Environmental Protection Agency (EPA) National Emissions Inventory (NEI). As described in Larkin et al. (2014), the US EPA NEI is produced every three years and includes state submitted data. For this study, the years 2011 and 2014 are NEI process years while the remaining years in this study are considered fire inventory data, which were compiled using a more limited set of inputs. Therefore, while the US EPA emissions data is referred to as NEI in this study, it is important to remember that only 2005, 2008, 2011 and 2014 are NEI process years and the remaining years are based on EPA fire inventory data. Furthermore, a regression analysis, using forward stepwise regression, was completed in order to determine the best fitting model of NH_3 emissions from biomass burning using a combination of in-situ and satellite (primarily NASA's Terra and Aqua) observations. This work proposes a new methodology to project emissions of NH_3 on a national scale, which would help society understand the implications of the changing climate and adequately prepare and/or prevent these changes. Furthermore, this methodology also provides a relatively simply approach to estimating past, present and future emissions based on readily accessible data (temperature and burn area).

2. Data & methodology

In order to compare the calculated fire emissions (discussed in the following section) with the fire properties (number of fires, fire radiative power, and fire brightness temperature) as well as to observe trends in the fire properties, the National Aeronautics and Space Administration's (NASA) Fire Information for Resource Management System (FIRMS) was utilized to obtain archived fire locations, frequency and strength. This data was obtained from the MODIS sensor on NASA's Earth Observing System satellites (Terra and Aqua) (Friedl et al., 2010). The MODIS active fire product obtained (Collection 6, Giglio et al., 2016) uses a fire detection algorithm that uses a multispectral contextual approach to leverage the mid-infrared radiations emitted by fires (Davies et al., 2009). FIRMS delivers the MODIS fire data locations that represent the center of a 1 km pixel that is flagged by the algorithm as an area that contains at least one fire/hotspot within the pixel (Davies et al., 2009). The brightness temperature is calculated using the average intensity of infrared radiation at two wavelengths near 4 μm for a 1 km × 1 km pixel (Giglio et al, 2003, 2016). In the Collection 6 MODIS active fire product, the fire radiative power was derived using the Wooster et al. (2003), Wooster et al. (2012) approach (Giglio et al., 2016). In order to ensure quality, only fire data with a confidence estimate greater than 33% (i.e. medium and high confidence fires) will be used in this study.

2.1. Quantification of NH_3 emissions

There are several methods that can be used to quantify emissions of pollutants (i.e. NH_3) from biomass burning (i.e. Van Der Werf et al., 2003; Hoelzemann et al., 2004; Ito and Penner, 2004; Van Der Werf et al., 2014; Dennis et al., 2002; Langmann et al., 2009; Ichoku and Ellison, 2014). In this study, ammonia emissions from biomass burning were calculated using the emission factor approach (Equation (1)) equation adapted from Seiler and Crutzen (1980), Wiedinmyer et al. (2006), Wiedinmyer et al. (2011) and Oliveras et al. (2014):

$$E_i = BA_{(x,t)} \times B_{(x)} \times FB \times EF_j \quad (1)$$

where E_i is the emission of species i (in this case, NH_3), BA is the area burned at time t and location x, B is the biomass loading at location x, FB is the fraction of that biomass burned in the fire and EF_i is the emission factor of species i. In order to obtain the area burned (BA), the Moderate Resolution Imaging Spectroradiometer (MODIS) Burned Area product (MCD45, Collection 5.1), obtained from the University of Maryland's website, was used. The burn area is determined by the MODIS algorithm that uses time series of the daily 500 m MODIS land surface reflectance data (Roy et al., 2002, 2005, 2008). The MODIS burned area product was validated by Roy et al. (2005) and then again by Roy and Boschetti (2009), who found that the MODIS product provided the most accurate burned area maps when compared with other products (i.e. L3JRC, GlobCarbon). The biomass loading (B), which is defined as the amount of biomass available that can be burned in each fire, was obtained from Table 1 in Wiedinmyer et al. (2006), which describes the total fuel loading assumptions for various land cover classifications based on the literature. In order to quantify the amount of biomass burned, it was first necessary to know the type of land being burned. Therefore, the Collection 5 MODIS Global Land Cover Type product for 2010 (MCD12Q1) was used to determine land type (Friedl et al., 2010; Channan et al., 2014). This database contains land cover classifications at a spatial resolution of 500 m. This data was readily

Table 1
The biomass loading term (kg m^{-2}) for each respective land classification type (Wiedinmyer et al., 2006) and the NH_3 emission factor for each land classification type (Wiedinmyer et al., 2011).

Land Classification	Biomass Loading (kg per m^2)	NH_3 Emission Factor (g per kg Biomass Burned)
Barren	0.1	0.49
Cropland	0.5	2.3
Deciduous Broadleaf Forest	9.5	1.5
Deciduous Needleleaf Forest	12	3.5
Evergreen Broadleaf Forest	17	0.76
Evergreen Needleleaf Forest	14	3.5
Grasslands	1.1	0.49
Mixed Forest	12	1.5
Open Shrublands	4.3	1.2
Closed Shrublands	4.3	1.2
Permanent Wetlands	1.1	0.49
Savannas	1.1	0.49
Woody Savannas	1.1	1.2
Snow/Ice	0	0
Urban	0.1	0
Water	0	0

available from the MRLC website. This was then used to estimate the fraction of biomass burned (FB) within the fire using the methods used by Wiedinmyer et al. (2006) and Wiedinmyer et al. (2011), which were adapted from Ito and Penner (2004). In this method, areas with 60% or more tree cover are given an FB value of 0.3 for the woody fuel and 0.9 for herbaceous cover. Areas with 40–60% tree covers, the FB is 0.3 for woody fuels and the FB for herbaceous fuels can be calculated using the following equation (Equation (2)):

$$FB_{herb} = e^{-0.13 * FractionTreeCover} \quad (2)$$

Finally, when the fraction of tree cover is less than 40%, no woody fuel is assumed to burn and an FB value of 0.98 is given for herbaceous fuels (Wiedinmyer et al., 2006; Ito and Penner, 2004). The fraction of tree cover was obtained at a 1 km^2 spatial resolution via the Advanced Very High Resolution Radiometer (AVHRR) Continuous Fields Tree Cover product, which was readily available from the University of Maryland (DeFries et al., 2000). The emission factor (EF) for ammonia was obtained from Wiedinmyer et al. (2011), who classified the emission factors based on MODIS land use/land cover classification based on literature values (Akagi et al. (2011) for the NH_3 emission factors). Table 1 shows the emission factors used in this study, obtained from Wiedinmyer et al. (2011).

As with most datasets, there are some limitations and uncertainties associated with the satellite products used in this study. While satellite datasets are extremely useful, there are some limitations associated with them, such as satellite overpass time and cloud cover. Some uncertainties associated with the MODIS burn area data include potential burn area underestimation due to canopy vegetation and/or cloud cover and difficulty mapping small fires (Roy and Boschetti, 2009). The biggest limitations with the AVHRR continuous tree product is its age (acquired 1992–1993). The accuracy of the land classifications for the MODIS Land Cover dataset is approximately 75% with an error variance on this estimate of 1.3% and a 95% confidence interval of 72.3–77.4% (Friedl et al., 2010). Furthermore, uncertainties can arise from natural variations in emission factors (Akagi et al., 2011).

2.2. Comparison with other inventories

In comparison with other inventories, the methodology used in this study most closely resemble the methodology used in FINN (Table 2), due to the usage of the MODIS Land Cover product biomass loading

Table 2
Comparison in methodology and input data used in this study with other accepted inventories.

	This Study	*FINN*	*NEI*	*GFED*
Burn Area	MODIS burn area product (MOD45)	MODIS thermal anomalies product	Incident reports, NOAA HMS fire products	MODIS burn area product (MCD64A1) with an estimation of small fires using active fire data
Biomass Loading	Lookup table [from Wiedinmyer et al. (2006)] using MODIS Land Cover (MCD12Q1) 2005 (preliminary results) and 2010 (future work)	Lookup table using MODIS Land Cover (MCD12Q1) 2005	Fuel characteristic classification system derived from Landsat	CASA model
Fraction of Biomass Burned	Function of % Tree Cover (AVHRR Continuous Tree Cover product [preliminary; for 1992/1993] and MODIS VCF [future work; for 2010])	Function of % Tree Cover (MODIS VCF product for 2001)	Estimated in consumption model	Lookup table with fraction for standing biomass, standing fuel and surface litter
Emission Factors	Akagi et al. (2011); Urbanski (2014); Andreae and Merlet (2001)	Akagi et al. (2011)	Wildfire based on Urbanski (2014); Agriculture based on Pouliot et al. (2017)	Akagi et al. (2011); Andreae and Merlet (2001)

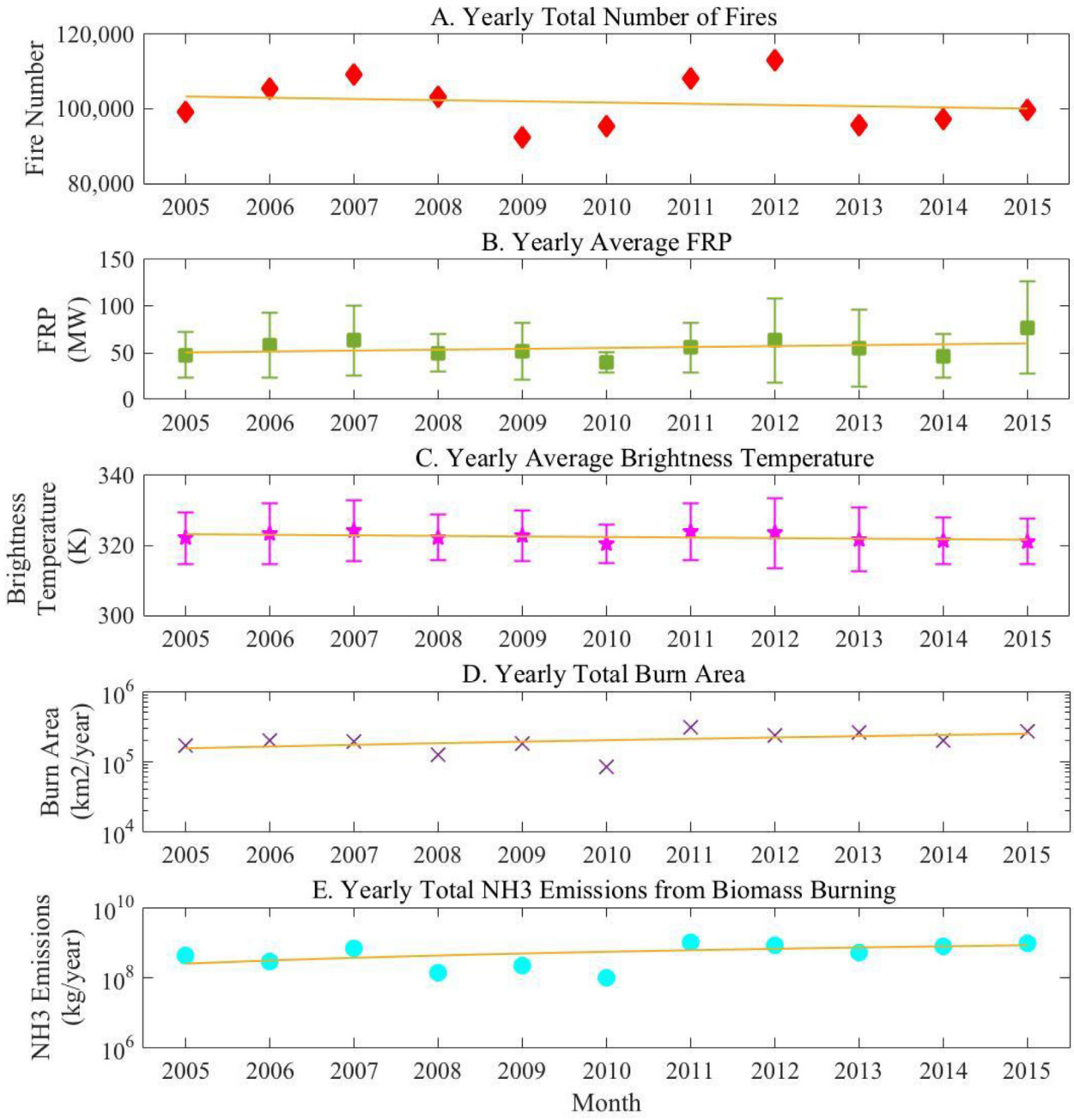

Fig. 1. The yearly total number of fires, the yearly average fire radiative power (and associated standard deviation), the yearly average brightness temperature (and associated standard deviation), the yearly burn area and the yearly ammonia emissions from fires plotted for 2010–2014. The associated trend line is displayed as a yellow-gold line. Error bars represent the standard deviation. (For interpretation of the references to colour in this figure legend, the reader is referred to the Web version of this article.)

lookup table from Wiedinmyer et al. (2006), the methodology used to determine the fraction of biomass burned and the emission factors used (i.e. Akagi et al., 2011). However, the input variables are different.

The US EPA NEI is produced every three years and includes a combination of methodologies. National processing is done using the methodology described below, but states are allowed to submit revised emissions that supersede the national processing. For wildland fires, national processing is done using estimations of the burned area of the fire, the available fuel, the fuel moisture conditions, and an emission factor for the pollutant for a specific land classification type. Wildland fire emissions are processed using a combination of the SmartFire2 fire information system and the BlueSky modeling framework (Larkin et al., 2010). For the 2011 and 2014 NEIs (EPA, 2016, 2015), area burned data were collected from the S/L/T (state, local, tribe) agencies as well as from national agencies and organizations and then cleaned (i.e. eliminating errors and standardizing format) and combined with satellite fire detections to produce a single comprehensive daily fire location data. Fuel loadings were taken from the Fire Characteristic Classification System (FCCS) (McKenzie et al., 2007). The fuel moisture taken from the Wildland Fire Information System using fire weather observation files from remote weather stations operated by the US Forest Service (USFS). The fire location, fuel moisture and fuel loading data is then used within the BlueSky Framework to estimate the fuel consumption and the smoke emissions using a consumption model. The emission factors used in the 2014 NEI estimation for wildland fires were regional emission factors based on the work of Urbanski (2014). For

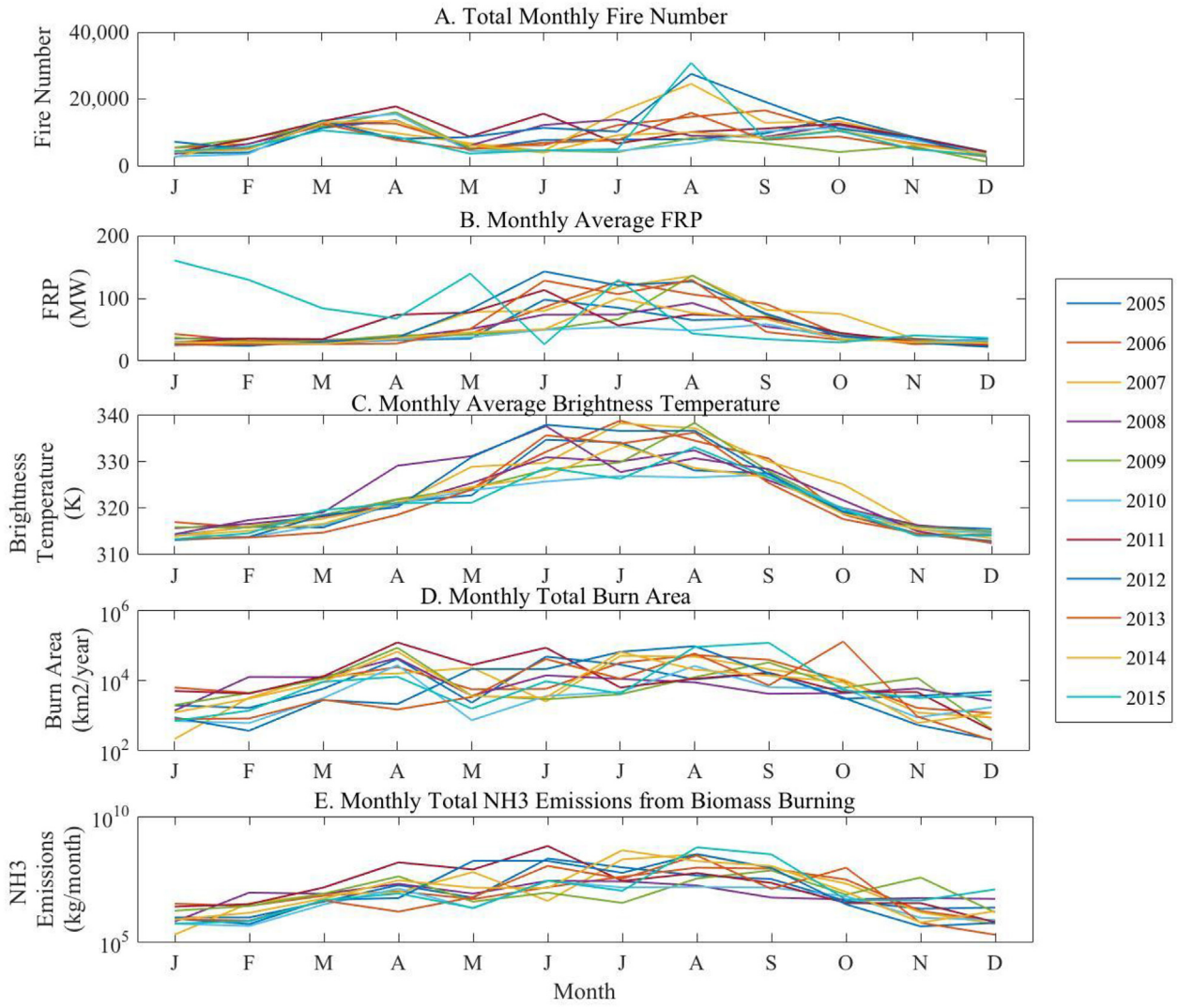

Fig. 2. The monthly total number of fires, the monthly average fire radiative power, the monthly burn area and the monthly NH_3 emissions from biomass burning for each year in the study.

agricultural burning, the NEI uses the Hazard Mapping System (HMS) fire product to detect fires and then extricates the agricultural fires and identifies the crop type using the USDA Cropland Data Later product (Pouliot et al., 2017). The emissions factors for ammonia used for the agricultural burning were derived from crop residue emission estimates from the 2002 NEI, which used a ratio of NH_3/NOx and the NOx emission factor (McCarty, 2011; Pouliot et al., 2017). When comparing the emission factors used for the US EPA NEI with the emission factors used in this study, there are similarities and differences in the categories. For example, while this study gives a specific emission factor for agriculture, the NEI uses a different emission factors for each specific type of cropland (Pouliot et al., 2017). In addition to this, it is important to note that while this study does not specify between prescribed fires and wildfire, the NEI does.

As is done in the methodology of this study, FINN also uses Equation (1) to estimate emissions from biomass burning (Wiedinmyer et al., 2006, 2011). However, there are some differences in data used between the two methods (Table 2). The default version of the FINN model identifies the location and the timing of fires using the MODIS Thermal Anomalies Product (Giglio et al., 2003, 2006), which detects active fires, at a nominal horizontal resolution of approximately 1 km^2, based on observations from the Moderate Resolution Imaging Spectroradiometer (MODIS) instruments on board of NASA's Terra and Aqua satellites. The processed fire detection data, which is processed via the MODIS Rapid Response or the MODIS Data Processing System (Collection 5), was obtained directly from the University of Maryland (Wiedinmyer et al., 2011). FINNv1 does not obtain the area burned using a burned area product. Instead, each fire is assumed a burn area of 1km^2, with grasslands assigned a burn area of 0.75 km^2 (Wiedinmyer et al., 2006, 2011; Al-Saadi et al., 2008). The MODIS Collection 5 Land Cover Type (LCT) product for 2005 (Friedl et al., 2010) is used to obtain the type of vegetation burned at each fire pixel. Each fire pixel is then assigned a land classification using the IGBP (International Geosphere-Biosphere Programme) land cover classification table. The MODIS Vegetation Continuous Fields (VCF) product (Collection 3 for 2001), which identifies the tree cover percent, the non-tree vegetation percent, and bare cover percent at a resolution of 500 m (Hansen et al.,2003, 2005), is used to determine the density of the vegetation at each fire pixel (Wiedinmyer et al., 2011). The land classification is then simplified such that all the land classification categories are lumped into 6 generic land classifications in order to make use easier with known emission factors and fuel loadings (Wiedinmyer et al., 2011). The fuel loadings used in FINN are based on the work of Hoelzemann et al. (2004), with updates made by Wiedinmyer et al. (2011). The fraction of biomass burned is obtained following the work of Ito and Penner (2004). While there are many similarities between the inputs of FINN

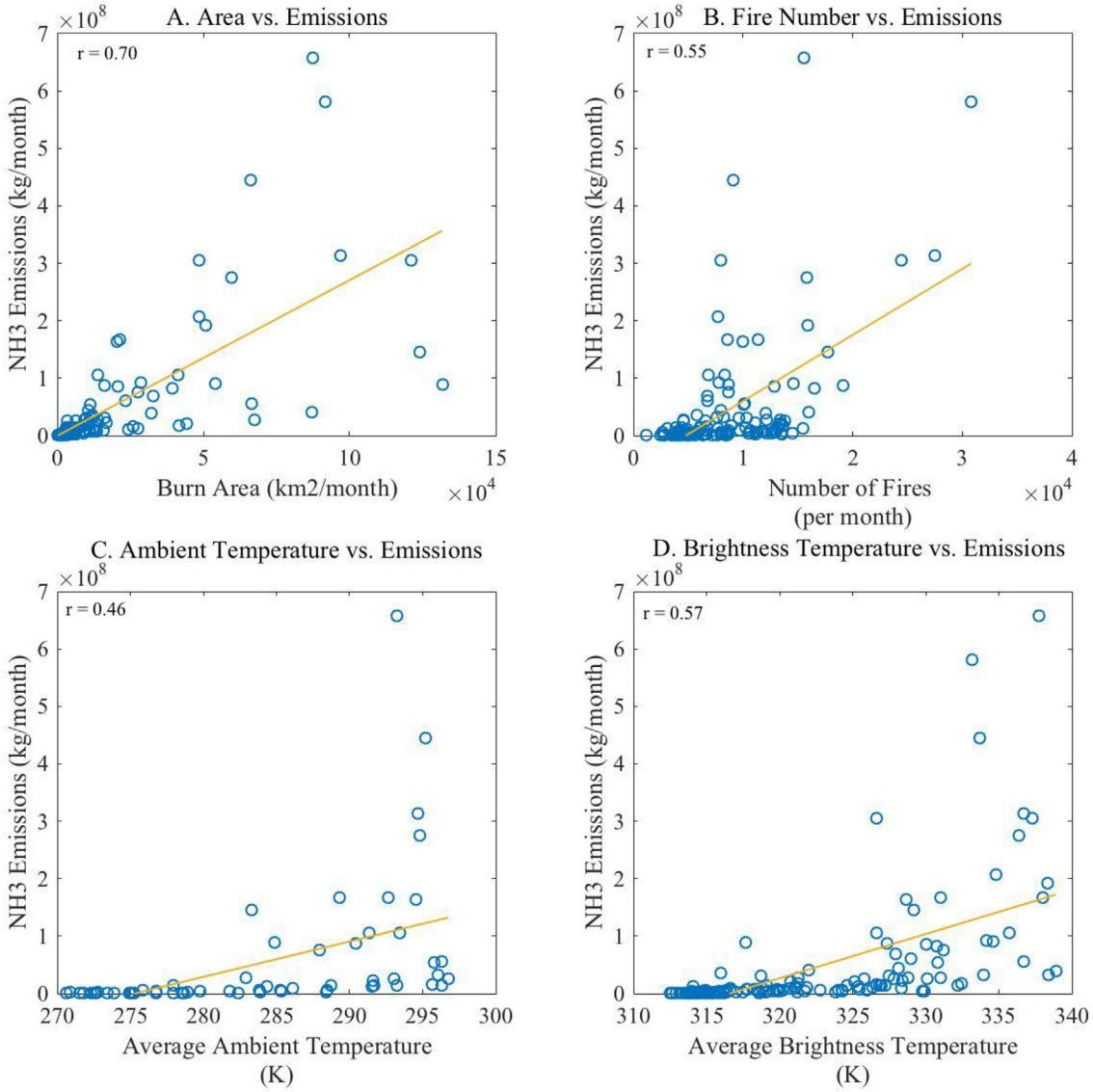

Fig. 3. Comparing the total monthly ammonia emissions (kg) from fires, represented by the circles, with the total monthly burn area (m^2) (A) for the continental United States, the number of fires (B), with the monthly average ambient temperature (C) and monthly average brightness temperature (D), plotted on a linear scale.

versus the calculations used in this study, such as the emission factors used, the land classification data used and the methodology for the fraction of biomass burned, there are also some major differences. For example, this study uses the MODIS burned area product for the burn area input as oppose to estimation technique based off the active fire data used in default runs of FINN. In addition to this, the fraction of biomass burned product used in this study (AVHRR Continuous Fields Tree Cover product) is different than what was used in FINN (MODIS Vegetation Continuous Fields (VCF) product) and the land classifications in this study were not simplified as they were done in FINN.

The GFED emissions of ammonia are estimated by combining the burned area data and emission factor data with a revised version of the Carnegie-Ames-Stanford Approach (CASA –GFED) biogeochemical model that estimates fuel loads and combustion completeness for each monthly time step (Van Der Werf et al., 2010; Van Der Werf et al., 2017). Within the CASA-GFED modeling framework, there are several different datasets used. The ambient air temperature, soil moisture and solar radiation data are obtained from European Center for Medium Range Weather Forecasts' ERA-Interim dataset, as described by Dee et al. (2011) (Van Der Werf et al., 2017). Other datasets include the fAPAR (fraction of absorbed Photosynthetically Active Radiation) data, which is used to estimate net primary production (NPP), calculated based on version 3 g of the Global Inventory Modeling and Mapping Studies (GIMMS) normalized difference vegetation index (NDVI) (Pinzon and Tucker, 2014), the fraction of tree cover (FTC) derived from the vegetation continuous fields MOD44B (V051) from MODIS (Hansen et al., 2005), and land classification data from MODIS MCD12C1 with classifications from the University of Maryland land cover classification dataset (Friedl et al., 2010). The burn area used in GFED is a combination of the 500 m Collection 5.1 MODIS direct broadcast (DB) burned area product (MCD64A1) at a spatial resolution of 0.25° (Giglio et al., 2013) and the burn are of small fires, which is statistically estimated using the 500 m burn area (MCD64A1), the active fire data from MODIS and 500 m surface reflectance observations (see Randerson et al., 2012 and van der Werf., 2017). The modeling framework calculates the carbon fluxes and then the emission factors are used to calculate these fluxes into emissions.

2.3. Regression analysis

Emissions of NH_3 from biomass burning are dependent upon not only fuel type and fire properties, but also meteorological conditions.

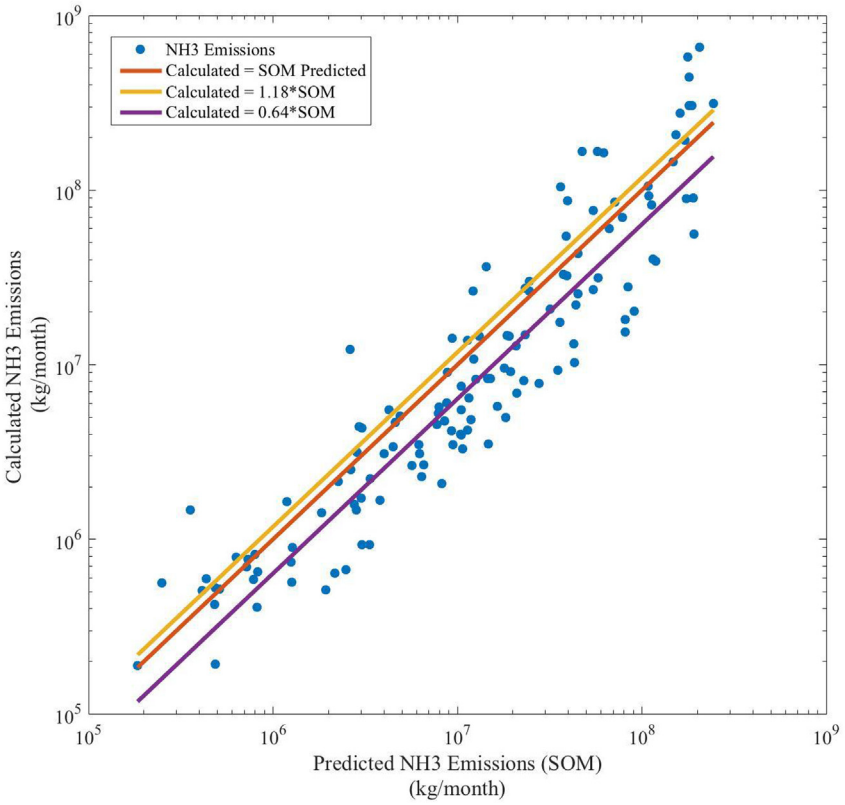

Fig. 4. Comparing the predicted NH_3 emissions with the calculated NH_3 emissions for 2010–2014 on a log scale. The red line represents the one-to-one trendline where the calculated NH_3 emissions = the predicted SOM NH_3 emissions. The gold line represents the mean bias line and the purple line represents the median bias line. (For interpretation of the references to colour in this figure legend, the reader is referred to the Web version of this article.)

Table 3
Comparison statistics for national monthly NH_3 emissions for 2010 to 2014.

	NH_3 Emissions (kg Month^{-1})
Observations	
Average	4.5e7
Standard Deviation	1.0e8
Max	6.5e8
Median	7.7e6
Model	
Average	3.8e7
Standard Deviation	5.5e7
Max	2.4e8
Median	1.2e7
Comparison Statistics	
Mean Normalized Bias (%)	69
Normalized Mean Bias (%)	−0.12
Normalized Mean Error (%)	0.44
Ratio of average measured value to average modeled value	1.18
Ratio of median measured value to median modeled value	0.64
Correlation Coefficient (r)	0.78
Number of Observations	132

Therefore, a statistical regression analysis was performed using SAS (v9.4) to determine a regression model to predict NH_3 emissions from biomass burning using the burn area and ambient air temperature. Using this data, the statistical observation model (SOM) ($r^2 = 0.92$, $n = 48$) for NH_3 emissions ($E_{NH3,}$ in g) is as follows (Equation (3)):

$$E_{NH3} = 0.012*[\ (BA^{0.88})\ *((T_A + 20)^{2.25})] \quad (3)$$

where BA is the total monthly burn area (m^2) and T_A is the average monthly ambient temperature (°C). The burned area data used in this regression analysis is described in the proceeding sections. The meteorological data (the average ambient temperature) were obtained from the National Oceanic and Atmospheric Administration (NOAA) National Centers for Environmental Information Climate Data website (Menne et al., 2012). The GHCND (Global Historical Climatology Network) Monthly Summary data for the CONUS from 2010 to 2013 were used, which provided the monthly mean temperature (°F). This data is described in detail in Menne et al. (2012). To ensure accuracy, only measurements that passed the NOAA National Climatic Data Center quality assurance check were used in this study. The emission inventory created in this study was used in the development of this regression analysis because it is easily reproducible using readily available satellite datasets (e.g. MODIS burn area and land cover data) for any emission species that emission factors have been developed for. It is important to note that several iterations were done in the creation of this regression equation using all and a combination of the following parameters: monthly total burn area, the monthly total number of fires, the monthly total precipitation, the average monthly temperature, the average monthly fire radiative power and the average monthly fraction of biomass burned and fuel loadings. While all of these are important parameters to estimate emissions from biomass burning, the equation with just burn area and temperature provided the best results (based on correlation coefficient and mean normalized bias).

2.4. Statistical comparison

There are several methods that can be used to evaluate air quality models (e.g EPA, 1991; Tong and Mauzerall, 2006). In this study, the mean normalized bias (MNB), the normalized mean bias (NMB) and the normalized mean error (NME) were used in the comparison between the NH_3 emissions from biomass burning calculated in this study and those emissions determined by the regression model in order to determine the accuracy of the model. The equations for the statistical comparisons are as follows:

$$MNB = \frac{1}{N}\sum_{i=1}^{N}\left(\frac{E_m(i) - E_c(i)}{E_{c\,(i)}}\right), \quad (4)$$

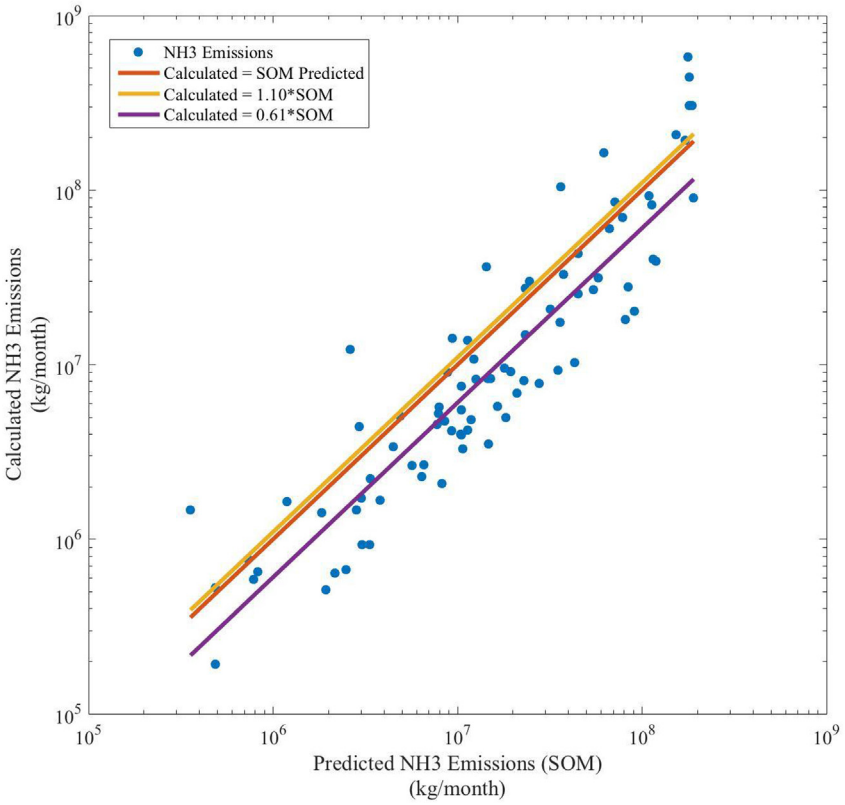

Fig. 5. Comparing the predicted NH_3 emissions with the calculated NH_3 emissions for 2014 on a log scale. The red line represents the one-to-one trendline where the calculated NH_3 emissions = the predicted SOM NH_3 emissions. The gold line represents the mean bias line and the purple line represents the median bias line. (For interpretation of the references to colour in this figure legend, the reader is referred to the Web version of this article.)

Table 4
Comparison statistics for the national monthly NH_3 emissions for 2014.

	NH_3 Emissions (kg Month^{-1})
Observations	
Average	4.2e7
Standard Deviation	9.5e7
Max	5.8e8
Median	8.2e7
Model	
Average	3.8e7
Standard Deviation	5.2e7
Max	1.9e8
Median	1.3e7
Comparison Statistics	
Mean Normalized Bias (%)	−91
Normalized Mean Bias (%)	−0.11
Normalized Mean Error (%)	0.72
Ratio of mean measured value to mean modeled value	1.10
Ratio of median measured value to median modeled value	0.61
Correlation Coefficient (r)	0.80
Number of Observations	84

$$NMB = \frac{1}{N}\frac{\sum_{i=1}^{N} E_m(i) - E_c(i)}{\sum_{i=1}^{N} E_c(i)}, \quad (5)$$

$$NME = \frac{1}{N}\frac{\sum_{i=1}^{N} |E_m(i) - E_c(i)|}{\sum_{i=1}^{N} |E_c(i)|}, \quad (6)$$

where N is the number of observations, E_m are the emissions projected by the regression model, and E_c are the emissions calculated in this study.

3. Results & discussion

On a national scale, there was a general decrease in the number of fires from 2005 to 2015, with an average change of ~2% per year (Fig. 1A). However, this trend is not statistically significant ($p > 0.05$, $R^2 = 0.03$). Over the period, there were, on average, 104,267 ± 16,461 fires per year, with the highest number of fires occurring in 2012 (132,469) and the lowest number of fires occurring in 2009 (81,149). When looking at the fire number per year on a monthly basis, there is a lot of variability year to year (Fig. 2A). However, on average, the monthly fire number peaks in both the spring and the fall. This bimodal, seasonal trend can likely be attributed to the agricultural burns that occur in the spring and the warm weather (which is conducive for fires) that occurs in the late summer. The yearly average fire radiative power, which measures the rate of the radiant heat output of a fire, showed a generally positive trend (average increase ~8% per year) on a national scale from 2005 to 2015. However, this trend was not statistically significant ($p > 0.05$, $R^2 = 0.1$). The average yearly FRP was 55 ± 10 MW, with the maximum average yearly FRP occurring in 2015 (77 ± 49 MW) and the minimum yearly average FRP occurring in 2010 (39 ± 10 MW) (Fig. 1B). On a monthly scale, FRP values generally peaked in the summer months, however, the highest monthly average FRP occurred in January of 2015 (160 MW) (Fig. 2B). The average yearly fire brightness temperature, which is a measure of the photons at a particular wavelength (4 μm) received by the spacecraft (Giglio et al., 2003; Giglio et al., 2016; NASA, 2018), was approximately constant (average −0.03% per year), with the yearly average brightness temperatures ranging from 320 K to 324 K (Fig. 1C). Similarly, the monthly average brightness temperatures were also approximately constant, ranging from 312 K to 339 K (Fig. 2C). On average, ~200,367 ± 64,112 km^2 of land was burned from 2005 to 2015, with highest total burn area occurring in 2011 (~305,449 km^2) and the lowest observed burn area occurring in 2010 (81,926 km^2) (Fig. 1D). While there was variation year to year in the total burn area, the general trend in area burned increased over the period (on average

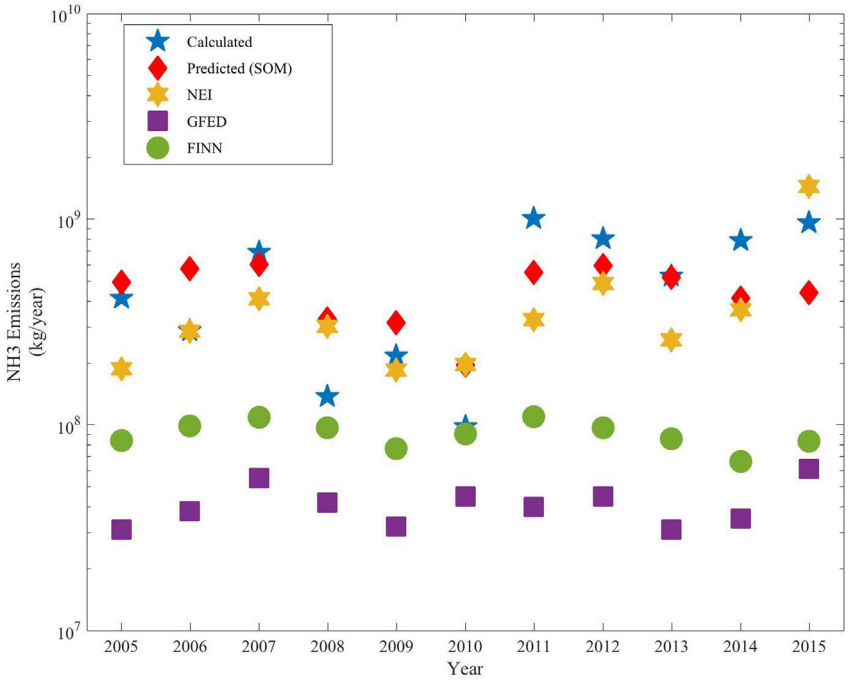

Fig. 6. Comparing the yearly total NH_3 emissions (on a log scale) from biomass burning calculated and predicted in this study with the NEI, the FINN and the GFED. Note that 2014 was not included in the creation of the SOM.

~23% per year). However, this trend was not statistically significant ($p > 0.05$, $R^2 = 0.2$). On a monthly scale, the peak burn area varies from year to year (Fig. 2D). However, it is evident that the peak burn area is at a maximum from May to September. This is expected due to the warmer and dryer conditions that occur in the North American spring and summer. It is important to note the limitation of the short study period. While the period is long enough to get a short term trend, a longer analysis time is needed to determine a definite trend.

3.1. Ammonia emissions from biomass burning

3.1.1. Calculated emissions

The average annual NH_3 emissions from biomass burning on a national scale were approximately 5.4e8 ± 3.3e8 kg $year^{-1}$ for 2005–2015. There was a general increase (on average ~98% per year) in the amount of ammonia emitted from biomass burning (Fig. 1E). However, this trend is statistically insignificant ($p > 0.05$, $R^2 = 0.3$). As discussed above, burn area is a key contributor to emissions of ammonia. The increase in burn area is important because a larger burn area likely leads to an increase in fuels (and available nitrogen) and therefore an increase in the ammonia emitted from the fires. Similar to the observed monthly burn area, there is variability for the monthly total emissions, particularly in the summer months (Fig. 2E). However, in general, NH_3 emissions tend to peak in the summer months. This can be attributed to wildland fire activity, which typically covers a larger burn area and occurs in the summer months when it is warmer and dryer (particularly in the western US), due to the nitrogen rich fuels (e.g. forests).

When comparing the number of fires and ammonia emissions from fires (Fig. 3B), a moderate positive relationship was observed ($r = 0.55$). When comparing ammonia emissions from fires with the burn area (Fig. 3A), a moderate-strong positive relationship was observed ($r = 0.70$). Because the inventory is built based on the burn area of fires as oppose to the number of fires, this was unsurprising. Similarly, moderate positive relationships were also observed when comparing the monthly average FRP (not shown) and brightness temperatures (Fig. 3D) with the average monthly NH_3 emissions ($r = 0.43$ and $r = 0.57$, respectively). A moderate positive relationship was observed when comparing ambient temperature with ammonia emissions ($r = 0.46$, Fig. 3C).

3.1.2. Regression analysis

A regression model that accounts for both fire size and meteorological conditions was created to predict monthly NH_3 emissions from biomass burning (Equation (3); $r^2 = 0.92$, $n = 48$). When comparing this model (SOM) against the monthly calculated emissions from this study (Fig. 4, Table 3), it was found that the regression model was a factor of 1.18 lower than the mean observed values and a factor of 0.64 higher than the median observed values. The aforementioned comparison statistics were done to compare the SOM against emissions calculated during this study. The mean normalized bias (MNB) was 69%, the normalized mean bias (NMB) was −0.12% and the normalized mean error (NME) was 0.44%. However, because much of the data (2010–2013) used to calculate the monthly emissions for this study were used in the creation of the regression model, this similarity between the model and the observations was expected. Therefore, to test the SOM further, the modeled emissions were then compared against the calculated emissions for 2005–2009 and 2015 (i.e. emissions not used in the creation of the regression). The results of this showed that the model was a factor of 1.10 lower than the mean calculated emissions and a factor of 0.61 higher than the median calculated emissions (Fig. 5, Table 4). The comparison statistics for this analysis showed that the MNB = 91%, the NMB = −0.11% and the NME = 0.72%.

3.2. Comparison with other inventories

Fig. 6 compares the results of this study with prominent emission inventories. There is a lot of variation both between each year as well as between each inventory. On a national scale, the calculated (average 5.40e8 ± 3.31e8 kg $year^{-1}$) and modeled (average 4.58e8 ± 1.33e8 kg $year^{-1}$) ammonia emissions from biomass burning were found to be, on average, a factor of 1.3 and 1.1, respectively, higher than the US EPA National Emissions Inventory (average 4.04e8 ± 3.57e8 kg $year^{-1}$) (EPA, 2016, 2015). Similar to the comparisons between the NEI and the

calculated ammonia emissions from biomass burning in this study, the total yearly ammonia emissions from biomass burning modeled by FINN (average 9.08e7 ± 1.33e7 kg year^{-1}) (Wiedinmyer et al., 2011) and the GFED (average 4.14e7 ± 9.77e6 kg year^{-1}) (Van Der Werf et al., 2017) were both lower than what was calculated in this study. On average, the emissions calculated and modeled in this study were a factor of 5.9 and 5.0, respectively, higher than the emissions obtained from FINN and a factor of 13.1 and 11.1 higher than those obtained from the GFED.

Through the study period, the NEI yearly total NH_3 emissions from biomass burning were consistently similar to both the calculated emissions and the SOM predicted emissions. Similarly, both FINN and GFED were consistently lower than both the NEI and the emissions quantified in this work. Despite using the same general methodology, the emissions between inventories are highly variable. Due to both uncertainties in NH_3 emissions from fires as well as uncertainties in the products used to obtain emission estimates, it is not surprising that there are major inconsistencies between each inventory. Variation between fire emission inventories was also observed by Larkin et al. (2014), who did a similar study comparing several pollutant emissions (e.g. CO_2, CH_4, N_2O) for CONUS from FINN, GFED, NEI and the EPA Greenhouse Gas emissions inventories. Similar trends were observed, where the NEI projected the highest emissions, followed by FINN and then GFED. The differences observed in Larkin et al. (2014) were attributed to the differences and uncertainties associated with the input parameters, such as how prescribed fires were represented, the fuel loadings used as well as how deep organic combustion was modeled. Variation in and uncertainties associated with all the input parameters for biomass burning emissions all contribute to disagreement between inventories. Furthermore, the magnitude of variation in reactive nitrogen emission inventories (including, but not limited to biomass burning emissions) is extreme due to uncertainties in the strength of the emission sources as shown by Battye et al. (2017).

4. Conclusions

According to the U.S. EPA's 2014 National Emission Inventory (EPA, 2014), biomass burning is the second largest emissions source of ammonia (accounting for ~10%) following agricultural sources. The results of this study showed that on average, there were 5.4e8 ± 3.3e8 kg of NH_3 year^{-1} emitted across the CONUS for 2005–2015. Through the study period, there was a general decrease in the number of fires and a general increase in the average fire radiative power, the total area burned and in the total ammonia emitted from biomass burning. However, these observed trends were not statistically significant.

A regression model ($r^2 = 0.92$, n = 48) was developed in order predict emissions as a function of fire burn area and ambient temperature. When comparing the regression model with the results from this study, it was found that the regression model was a factor of 1.18 (MNB = −69%, NMB = −0.12%, NME = 0.44%) lower than what was observed. Both the calculated and modeled (i.e. predicted by the statistical regression model) NH_3 emissions were then compared against currents fire emission inventories (NEI, FINN, GFED). When comparing the US EPA National Emissions Inventory for NH3 emissions from fires for the continental United States, it was found that the NEI was approximately a factor of 1.3 and 1.1 lower than what was calculated and modeled, respectively, in this study. Similarly, the emissions calculated and modeled in this study were a factor of 5.9 and 5.0, respectively, higher than the emissions obtained from FINN and a factor of 13.1 and 11.1 higher than those obtained from the GFED. These discrepancies are attributed to differences in the emission estimation technique used as well as differences in the input data used.

4.1. Future work

Due to the short nature of this study, the next step is to extend the study period in order to conduct a better trend analysis. Furthermore, the data used to determine the fraction of biomass burned will be updated from the AVHRR Continuous Fields Tree Cover Product to the MODIS Vegetation Continuous Fields product. This will allow for a more accurate estimate of the fraction of biomass burned. Changes in the earth's climate will likely influence both fire strength and frequency, and therefore influence emissions of ammonia from biomass burning. An increase in emissions from fires could potentially lead to higher concentrations of ammonia. The statistical regression model developed in this study will allow for the prediction of ammonia emissions associated with future climate change. Future directions with this work include projecting ammonia emissions using future climate scenarios in order to see how emissions will change as the climate changes.

Acknowledgements

The authors would like to acknowledge the University of Maryland, Department of Geography, and NASA for generously providing their data for all to use on the UMD website. We would also like to thank Dr. David Dickey for all his help and guidance with the statistics used in this study. Moreover, we would also like to thank Dr. Charles Ichoku (NASA); Dr. Venkatesh Rao, Dr. Madeleine Strum and the US EPA Emission Inventory and Analysis Group; and Dr. Christine Wiedinmyer and the NCAR ACCORD Fire Data Analysis Workshop for their generous help and guidance provided for this work as well as for the travel support provided for CDB to participate in the ACCORD Fire Data Analysis Workshop, which was greatly appreciated. Daniel Tong and Pius Lee acknowledge support from NASA Applied Science Program (Grant # NNX16AQ19G). Finally, the authors would like to extend a special thank you to Dr. Sim Larkin, US Forest Service, for his extensive and extremely helpful comments on the manuscript.

References

Akagi, S., Yokelson, R.J., Wiedinmyer, C., Alvarado, M., Reid, J., Karl, T., Crounse, J., Wennberg, P., 2011. Emission factors for open and domestic biomass burning for use in atmospheric models. Atmos. Chem. Phys. 11, 4039–4072.

Al-Saadi, J., Soja, A.J., Pierce, R.B., Szykman, J., Wiedinmyer, C., Emmons, L., Kondragunta, S., Zhang, X., Kittaka, C., Schaack, T., 2008. Intercomparison of near-real-time biomass burning emissions estimates constrained by satellite fire data. J. Appl. Remote Sens. 2 021504–021504-24.

Alves, C.A., Vicente, A., Monteiro, C., Gonçalves, C., Evtyugina, M., Pio, C., 2011. Emission of trace gases and organic components in smoke particles from a wildfire in a mixed-evergreen forest in Portugal. Sci. Total Environ. 409, 1466–1475.

Andreae, M.O., Merlet, P., 2001. Emission of trace gases and aerosols from biomass burning. Global Biogeochem. Cycles 15, 955–966.

Aneja, V.P., Murray, G., Southerland, J., 1998. Atmospheric nitrogen compounds: emissions, transport, transformation, deposition, and assessment. J. EM 22–25.

Aneja, V.P., Schlesinger, W.H., Erisman, J.W., 2008. Farming pollution. Nat. Geosci. 1, 409–411.

Aneja, V.P., Schlesinger, W.H., Erisman, J.W., 2009. Effects of agriculture upon the air quality and climate: research, policy, and regulations. Environ. Sci. Technol. 43, 4234–4240.

Baek, B.H., Aneja, V.P., 2004. Measurement and analysis of the relationship between ammonia, acid gases, and fine particles in eastern North Carolina. J. Air Waste Manag. Assoc. 54, 623–633.

Baek, B.H., Aneja, V.P., Tong, Q., 2004. Chemical coupling between ammonia, acid gases, and fine particles. Environ. Pollut. 129, 89–98.

Battye, W., Aneja, V.P., Schlesinger, W.H., 2017. Is nitrogen the next carbon? Earth's Future 5, 894–904.

Battye, W., Aneja, V.P., Roelle, P.A., 2003. Evaluation and improvement of ammonia emissions inventories. Atmos. Environ. 37, 3873–3883.

Behera, S.N., Sharma, M., 2010a. Investigating the potential role of ammonia in ion chemistry of fine particulate matter formation for an urban environment. Sci. Total Environ. 408, 3569–3575.

Behera, S.N., Sharma, M., 2010b. Reconstructing primary and secondary components of PM2. 5 composition for an urban atmosphere. Aerosol. Sci. Technol. 44, 983–992.

Bouwman, A., Lee, D., Asman, W., Dentener, F., Van Der Hoek, K., Olivier, J., 1997. A global high-resolution emission inventory for ammonia. Global Biogeochem. Cycles 11, 561–587.

Bouwman, A., 1996. Direct emission of nitrous oxide from agricultural soils. Nutrient Cycl. Agroecosyst. 46, 53–70.

Butler, T., Vermeylen, F., Lehmann, C., Likens, G., Puchalski, M., 2016. Increasing ammonia concentration trends in large regions of the USA derived from the NADP/

AMoN network. Atmos. Environ. 146, 132–140.
Channan, S., Collins, K., Emanuel, W., 2014. Global Mosaics of the Standard MODIS Land Cover Type Data. University of Maryland and the Pacific Northwest National Laboratory, College Park, Maryland, USA, pp. 30.
Chen, X., Day, D., Schichtel, B., Malm, W., Matzoll, A.K., Mojica, J., McDade, C.E., Hardison, E.D., Hardison, D.L., Walters, S., 2014. Seasonal ambient ammonia and ammonium concentrations in a pilot IMPROVE NHx monitoring network in the western United States. Atmos. Environ. 91, 118–126.
Clark, C.M., Tilman, D., 2008. Loss of plant species after chronic low-level nitrogen deposition to prairie grasslands. Nature 451, 712–715.
Crouse, D.L., Peters, P.A., van Donkelaar, A., Goldberg, M.S., Villeneuve, P.J., Brion, O., Khan, S., Atari, D.O., Jerrett, M., Pope III, C.A., 2015. Risk of Non-accidental and Cardiovascular Mortality in Relation to Long-term Exposure to Low Concentrations of Fine Particulate Matter: a Canadian National-level Cohort Study, vol. 120 (5), 708.
Davidson, E., David, M.B., Galloway, J.N., Goodale, C.L., Haeuber, R., Harrison, J.A., Howarth, R.W., Jaynes, D.B., Lowrance, R.R., Thomas, N.B., 2011. Excess nitrogen in the US environment: trends, risks, and solutions. Issues in Ecol. 15.
Davies, D.K., Ilavajhala, S., Wong, M.M., Justice, C.O., 2009. Fire information for resource management system: archiving and distributing MODIS active fire data. IEEE Trans. Geosci. Rem. Sens. 47, 72–79.
Day, D., Chen, X., Gebhart, K., Carrico, C., Schwandner, F., Benedict, K., Schichtel, B., Collett, J., 2012. Spatial and temporal variability of ammonia and other inorganic aerosol species. Atmos. Environ. 61, 490–498.
Dee, D.P., Uppala, S.M., Simmons, A.J., Berrisford, P., Poli, P., Kobayashi, S., Bechtold, P., 2011. The ERA-Interim reanalysis: configuration and performance of the data assimilation system. Q. J. R. Meteorol. Soc. 137 (656), 553–597.
DeFries, R., Hansen, M., Townshend, J., 2000. Global continuous fields of vegetation characteristics: a linear mixture model applied to multi-year 8 km AVHRR data. Int. J. Rem. Sens. 21, 1389–1414.
Dennis, A., Fraser, M., Anderson, S., Allen, D., 2002. Air pollutant emissions associated with forest, grassland, and agricultural burning in Texas. Atmos. Environ. 36, 3779–3792.
Erisman, J.W., Sutton, M.A., Galloway, J., Klimont, Z., Winiwarter, W., 2008. How a century of ammonia synthesis changed the world. Nat. Geosci. 1, 636–639.
Erisman, J.W., Galloway, J.N., Seitzinger, S., Bleeker, A., Dise, N.B., Petrescu, A.M., Leach, A.M., de Vries, W., 2013. Consequences of human modification of the global nitrogen cycle. Philos. Trans. R. Soc. Lond. Ser. B Biol. Sci. 368, 20130116.
Fan, J., Zhang, R., Li, G., Nielsen-Gammon, J., Li, Z., 2005. Simulations of fine particulate matter ($PM_{2.5}$) in Houston, Texas. J. Geophys. Res.: Atmos. 110, D16.
Flechard, C., Fowler, D., 1998. Atmospheric ammonia at a moorland site. I: the meteorological control of ambient ammonia concentrations and the influence of local sources. Q. J. R. Meteorol. Soc. 124, 733–757.
Friedl, M.A., Sulla-Menashe, D., Tan, B., Schneider, A., Ramankutty, N., Sibley, A., Huang, X., 2010. MODIS collection 5 global land cover: algorithm refinements and characterization of new datasets. Rem. Sens. Environ. 114, 168–182.
Galloway, J.N., Dentener, F.J., Capone, D.G., Boyer, E.W., Howarth, R.W., Seitzinger, S.P., Asner, G.P., Cleveland, C., Green, P., Holland, E., 2004. Nitrogen cycles: past, present, and future. Biogeochemistry 70, 153–226.
Giglio, L., Schroeder, W., Justice, C.O., 2016. The collection 6 MODIS active fire detection algorithm and fire products. Rem. Sens. Environ. 178, 31–41.
Giglio, L., Randerson, J.T., Werf, G.R., 2013. Analysis of daily, monthly, and annual burned area using the fourth-generation global fire emissions database (GFED4). J. Geophys. Res.: Biogeosciences 118, 317–328.
Giglio, L., Van der Werf, G., Randerson, J., Collatz, G., Kasibhatla, P., 2006. Global estimation of burned area using MODIS active fire observations. Atmos. Chem. Phys. 6, 957–974.
Giglio, L., Descloitres, J., Justice, C.O., Kaufman, Y.J., 2003. An enhanced contextual fire detection algorithm for MODIS. Rem. Sens. Environ. 87, 273–282.
Gillett, N., Weaver, A., Zwiers, F., Flannigan, M., 2004. Detecting the effect of climate change on Canadian forest fires. Geophys. Res. Lett. 31, 18.
Goode, J.G., Yokelson, R.J., Ward, D.E., Susott, R.A., Babbitt, R.E., Davies, M.A., Hao, W.M., 2000. Measurements of excess O_3, CO_2, CO, CH_4, C_2H_4, C_2H_2, HCN, NO, NH_3, HCOOH, CH_3COOH, HCHO, and CH_3OH in 1997 Alaskan biomass burning plumes by airborne Fourier transform infrared spectroscopy (AFTIR). J. Geophys. Res.: Atmos. 105, 22147–22166.
Hansen, M.C., Townshend, J.R., DeFries, R.S., Carroll, M., 2005. Estimation of tree cover using MODIS data at global, continental and regional/local scales. Int. J. Rem. Sens. 26, 4359–4380.
Hansen, M., DeFries, R., Townshend, J., Carroll, M., Dimiceli, C., Sohlberg, R., 2003. Global percent tree cover at a spatial resolution of 500 meters: first results of the MODIS vegetation continuous fields algorithm. Earth Interact. 7, 1–15.
Heald, C.L., JL Jr., C., Lee, T., Benedict, K., Schwandner, F., Li, Y., Clarisse, L., Hurtmans, D., Van Damme, M., Clerbaux, C., 2012. Atmospheric ammonia and particulate inorganic nitrogen over the United States, vol. 12 (21), 10295–10312.
Hoelzemann, J.J., Schultz, M.G., Brasseur, G.P., Granier, C., Simon, M., 2004. Global wildland fire emission model (GWEM): evaluating the use of global area burnt satellite data. J. Geophys. Res.: Atmos. 109 (D14).
Holtgrieve, G.W., Schindler, D.E., Hobbs, W.O., Leavitt, P.R., Ward, E.J., Bunting, L., Chen, G., Finney, B.P., Gregory-Eaves, I., Holmgren, S., Lisac, M.J., Lisi, P.J., Nydick, K., Rogers, L.A., Saros, J.E., Selbie, D.T., Shapley, M.D., Walsh, P.B., Wolfe, A.P., 2011. A coherent signature of anthropogenic nitrogen deposition to remote watersheds of the northern hemisphere. Science (New York, N.Y.) 334, 1545–1548.
Ichoku, C., Ellison, L., 2014. Global top-down smoke-aerosol emissions estimation using satellite fire radiative power measurements. Atmos. Chem. Phys. 14, 6643–6667.
Ito, A., Penner, J.E., 2004. Global estimates of biomass burning emissions based on satellite imagery for the year 2000. J. Geophys. Res.: Atmos. 109.
Janssens, I., Dieleman, W., Luyssaert, S., Subke, J., Reichstein, M., Ceulemans, R., Ciais, P., Dolman, A.J., Grace, J., Matteucci, G., 2010. Reduction of forest soil respiration in response to nitrogen deposition. Nat. Geosci. 3, 315–322.
Kwok, R., Napelenok, S., Baker, K., 2013. Implementation and evaluation of $PM_{2.5}$ source contribution analysis in a photochemical model. Atmos. Environ. 80, 398–407.
Langford, A., Fehsenfeld, F., Zachariassen, J., Schimel, D., 1992. Gaseous ammonia fluxes and background concentrations in terrestrial ecosystems of the United States. Global Biogeochem. Cycles 6, 459–483.
Langmann, B., Duncan, B., Textor, C., Trentmann, J., van der Werf, Guido R., 2009. Vegetation fire emissions and their impact on air pollution and climate. Atmos. Environ. 43, 107–116.
Larkin, N.K., Raffuse, S.M., Strand, T.M., 2014. Wildland fire emissions, carbon, and climate: US emissions inventories. For. Ecol. Manag. 317, 61–69.
Larkin, N.K., O'Neill, S.M., Solomon, R., Raffuse, S., Strand, T., Sullivan, D.C., Krull, C., Rorig, M., Peterson, J., Ferguson, S.A., 2010. The BlueSky smoke modeling framework. Int. J. Wildland Fire 18, 906–920.
Lelieveld, J., Evans, J., Fnais, M., Giannadaki, D., Pozzer, A., 2015. The contribution of outdoor air pollution sources to premature mortality on a global scale. Nature 525, 367–371.
Litschert, S.E., Brown, T.C., Theobald, D.M., 2012. Historic and future extent of wildfires in the southern Rockies ecoregion, USA. For. Ecol. Manag. 269, 124–133.
Liu, Y., Goodrick, S.L., Stanturf, J.A., 2013. Future US wildfire potential trends projected using a dynamically downscaled climate change scenario. For. Ecol. Manag. 294, 120–135.
Liu, Y., Stanturf, J., Goodrick, S., 2010. Trends in global wildfire potential in a changing climate. For. Ecol. Manag. 259, 685–697.
Liu, Y., 2006. North pacific warming and intense northwestern US wildfires. Geophys. Res. Lett. 33.
McCarty, J.L., 2011. Remote sensing-based estimates of annual and seasonal emissions from crop residue burning in the contiguous United States. J. Air Waste Manag. Assoc. 1, 22–34.
McKenzie, D., Raymond, C., Kellogg, L., Norheim, R., Andreu, A., Bayard, A., Kopper, K., Elman, E., 2007. Mapping fuels at multiple scales: landscape application of the fuel characteristic classification system this article is one of a selection of papers published in the special forum on the fuel characteristic classification system. Can. J. For. Res. 37, 2421–2437.
McMeeking, G.R., Kreidenweis, S.M., Baker, S., Carrico, C.M., Chow, J.C., Collett, J.L., Hao, W.M., Holden, A.S., Kirchstetter, T.W., Malm, W.C., 2009. Emissions of trace gases and aerosols during the open combustion of biomass in the laboratory. J. Geophys. Res.: Atmosphere 114 (D19).
Menne, M.J., Durre, I., Vose, R.S., Gleason, B.E., Houston, T.G., 2012. An overview of the global historical climatology network-daily database. J. Atmos. Ocean. Technol. 29, 897–910.
Nance, J.D., Hobbs, P.V., Radke, L.F., Ward, D.E., 1993. Airborne measurements of gases and particles from an Alaskan wildfire. J. Geophys. Res.: Atmos. 98, 14873–14882.
NASA, 2018. FIRMS FAQ. https://earthdata.nasa.gov/firms-faq, Accessed date: 5 April 2018.
Oliveras, I., Anderson, L.O., Malhi, Y., 2014. Application of remote sensing to understanding fire regimes and biomass burning emissions of the tropical Andes. Global Biogeochem. Cycles 28, 480–496.
Phoenix, G.K., Emmett, B.A., Britton, A.J., Caporn, S.J., Dise, N.B., Helliwell, R., Jones, L., Leake, J.R., Leith, I.D., Sheppard, L.J., 2012. Impacts of atmospheric nitrogen deposition: responses of multiple plant and soil parameters across contrasting ecosystems in long-term field experiments. Global Change Biol. 18, 1197–1215.
Piñol, J., Terradas, J., Lloret, F., 1998. Climate warming, wildfire hazard, and wildfire occurrence in coastal eastern Spain. Climatic Change 38, 345–357.
Pinzon, J.E., Tucker, C.J., 2014. A non-stationary 1981–2012 AVHRR NDVI3g time series. Rem. Sens. 6, 6929–6960.
Pope III, C.A., Ezzati, M., Dockery, D.W., 2009. Fine-particulate air pollution and life expectancy in the United States. N. Engl. J. Med. 360, 376–386.
Pope III, C.A., Burnett, R.T., Thun, M.J., Calle, E.E., Krewski, D., Ito, K., Thurston, G.D., 2002. Lung cancer, cardiopulmonary mortality, and long-term exposure to fine particulate air pollution. Jama 287, 1132–1141.
Pouliot, G., Rao, V., McCarty, J., Soja, A., 2017. Crop residue and rangeland burning in the 2014 National Emissions Inventory. to be submitted.
Pyne, S.J., Andrews, P.L., Laven, R.D., 1996. Introduction to Wildland Fire. John Wiley and Sons.
Randerson, J., Chen, Y., Werf, G., Rogers, B., Morton, D., 2012. Global burned area and biomass burning emissions from small fires. J. Geophys. Res.: Biogeosci. 117.
Reinhard, M., Rebetez, M., Schlaepfer, R., 2005. Recent climate change: rethinking drought in the context of forest fire research in Ticino, south of Switzerland. Theor. Appl. Climatol. 82, 17–25.
R'Honi, Y., Clarisse, L., Clerbaux, C., Hurtmans, D., Duflot, V., Turquety, S., Ngadi, Y., Coheur, P., 2013. Exceptional emissions of NH_3 and HCOOH in the 2010 Russian wildfires. Atmos. Chem. Phys. 13, 4171–4181.
Robarge, W.P., Walker, J.T., McCulloch, R.B., Murray, G., 2002. Atmospheric concentrations of ammonia and ammonium at an agricultural site in the southeast United States. Atmos. Environ. 36, 1661–1674.
Roy, D.P., Boschetti, L., 2009. Southern Africa validation of the MODIS, L3JRC, and GlobCarbon burned-area products. IEEE Trans. Geosci. Rem. Sens. 47, 1032–1044.
Roy, D.P., Boschetti, L., Justice, C.O., Ju, J., 2008. The collection 5 MODIS burned area product—global evaluation by comparison with the MODIS active fire product. Rem. Sens. Environ. 112, 3690–3707.
Roy, D., Jin, Y., Lewis, P., Justice, C., 2005. Prototyping a global algorithm for systematic fire-affected area mapping using MODIS time series data. Rem. Sens. Environ. 97, 137–162.

Roy, D., Lewis, P., Justice, C., 2002. Burned area mapping using multi-temporal moderate spatial resolution data—a bi-directional reflectance model-based expectation approach. Rem. Sens. Environ. 83, 263–286.
Saylor, R., Myles, L., Sibble, D., Caldwell, J., Xing, J., 2015. Recent trends in gas-phase ammonia and $PM_{2.5}$ ammonium in the southeast United States. J. Air Waste Manag. Assoc. 65, 347–357.
Schlesinger, W.H., Hartley, A.E., 1992. A global budget for atmospheric NH_3. Biogeochemistry 15, 191–211.
Schwartz, J., Laden, F., Zanobetti, A., 2002. The concentration-response relation between PM(2.5) and daily deaths. Environ. Health Perspect. 110, 1025–1029.
Seiler, W., Crutzen, P.J., 1980. Estimates of gross and net fluxes of carbon between the biosphere and the atmosphere from biomass burning. Climatic Change 2, 207–247.
Skibba, R., 2015. Assessing U.S. fire risks using soil moisture satellite data. EOSAccessed December 2016. https://eos.org/articles/assessing-u-s-fire-risks-using-soil-moisture-satellite-data.
Tong, D.Q., Mauzerall, D.L., 2006. Spatial variability of summertime tropospheric ozone over the continental United States: implications of an evaluation of the CMAQ model. Atmos. Environ. 40, 3041–3056.
Urbanski, S., 2014. Wildland fire emissions, carbon, and climate: emission factors. For. Ecol. Manag. 317, 51–60.
US EPA, 2016. 2014 National Emissions Inventory, Version 1 Technical Supporting Document. 4-73-7-1. United States Environmental Protection Agency, Research Triangle Park, NC 27711.
US EPA, 2015. 2011 National Emissions Inventory, Version 2. Technical Support Document. 323-348. United States Environmental Protection Agency, Research Triangle Park, NC 27711.
US EPA, 2014. 2014 National Emissions Inventory. United States Environmental Protection Agency, Research Triangle Park, NC 27711. http://www3.epa.gov/ttnchie1/net/2014inventory.html, Accessed date: June 2017.
US EPA, 1991. Guidance for Regulatory Application of the Urban Airshed Model. EPA-450/4-91-013, July 1991. United States Environmental Protection Agency, Research Triangle Park, NC 27711.
Van Der Werf, G., Randerson, J., Giglio, L., Chen, Y., Rogers, B., Van Leeuwen, T., 2014. Global fire emissions database version 4 (GFED4). In: AGU Fall Meeting Abstracts, 0545.
Van Der Werf, Guido R., Randerson, J.T., Giglio, L., Van Leeuwen, T.T., Chen, Y., Rogers, B.M., Mu, M., Van Marle, M.J., Morton, D.C., Collatz, G.J., 2017. Global fire emissions estimates during 1997–2016. Earth Syst. Sci. Data 9, 697.
Van Der Werf, Guido R., Randerson, J.T., Giglio, L., Collatz, G., Mu, M., Kasibhatla, P.S., Morton, D.C., DeFries, R., Jin, Y.v, van Leeuwen, T.T., 2010. Global fire emissions and the contribution of deforestation, savanna, forest, agricultural, and peat fires (1997–2009). Atmos. Chem. Phys. 10, 11707–11735.
Van Der Werf, Guido R., Randerson, J.T., Collatz, G.J., Giglio, L., 2003. Carbon emissions from fires in tropical and subtropical ecosystems. Global Change Biol. 9, 547–562.
Wang, X., Wang, W., Yang, L., Gao, X., Nie, W., Yu, Y., Xu, P., Zhou, Y., Wang, Z., 2012. The secondary formation of inorganic aerosols in the droplet mode through heterogeneous aqueous reactions under haze conditions. Atmos. Environ. 63, 68–76.
Westerling, A.L., Hidalgo, H.G., Cayan, D.R., Swetnam, T.W., 2006. Warming and earlier spring increase western U.S. forest wildfire activity. Science (New York, N.Y.) 313, 940–943.
Wiedinmyer, C., Akagi, S., Yokelson, R.J., Emmons, L., Al-Saadi, J., Orlando, J., Soja, A., 2011. The fire INventory from NCAR (FINN): a high resolution global model to estimate the emissions from open burning. Geosci. Model Dev. (GMD) 4, 625.
Wiedinmyer, C., Quayle, B., Geron, C., Belote, A., McKenzie, D., Zhang, X., O'Neill, S., Wynne, K.K., 2006. Estimating emissions from fires in north America for air quality modeling. Atmos. Environ. 40, 3419–3432.
Wooster, M.J., Xu, W., Nightingale, T., 2012. Sentinel-3 SLSTR active fire detection and FRP product: pre-launch algorithm development and performance evaluation using MODIS and ASTER datasets. Rem. Sens. Environ. 120, 236–254.
Wooster, M., Zhukov, B., Oertel, D., 2003. Fire radiative energy for quantitative study of biomass burning: derivation from the BIRD experimental satellite and comparison to MODIS fire products. Rem. Sens. Environ. 86, 83–107.
Yao, X., Zhang, L., 2016. Trends in atmospheric ammonia at urban, rural, and remote sites across north America. Atmos. Chem. Phys. 16, 11465–11475.
Zbieranowski, A.L., Aherne, J., 2012. Spatial and temporal concentration of ambient atmospheric ammonia in southern ontario, Canada. Atmos. Environ. 62, 441–450.